Chalcogenide Letters Vol. 21, No. 5, May 2024, p. 385- 394

Influence of annealing temperature on nano crystalline description for CuZnS thin films

A. J. Soud, Bushra K. H. Al-Maiyaly
Department of physics, College of Education For Pure Science (Ibn Al-Haitham), University of Baghdad, Baghdad, Iraq

Copper Zinc Sulphide ($Cu_{0.5}Zn_{0.5}S$) alloy and thin films were fabricated in a vacuum. Nano crystallized (CZS) film with thick 450±20 nm was deposit at substrates glasses using thermal evaporation technique below ~ 2×10^{-5} mbar vacuum to investigated the films structural, morphological and optical properties depended on annealing temperatures (as-deposited, 423, 523 and 623) K for one hour. The influences annealed temperature on structurally besides morphologically characteristics on these films were investigated using XRD and AFM respectively. XRD confirms the formation a mixed hexagonal phase of CuS-ZnS in (102) direction with polycrystalline in nature having very fine crystallites size varying from (5.5-13.09) nm. AFM analysis shows the uniform distribution of closely packed grains, grain size for that film diverge on ranges as of (52.37 to 89.25) nm after annealed. The optical properties of all films prepared had been examined for the wavelength range 400 - 1000 nm using UV-Vis-NIR spectrometer. The band gaps of ($Cu_{0.5}Zn_{0.5}S$) films are obtained in the range of 2.4 to 1.9 eV, which makes it a suitable absorber as well as buffer/window layer for solar cell applications.

(Received January 30, 2024; Accepted May 7, 2024)

Keywords: Copper zinc sulphide, AFM analysis, Annealing, Thermally evaporation

1. Introduction

Inordinate agreement attention had be interested for growths Nano composites film where could practical for absorbed on solar cells then optoelectronic apply [1]. Copper (Cu) Zinc (Zn) Sulfide (S) inexpensive elements, earth-abundant, and non-toxic mutual by appropriate optically plus electrically property were talented applicant by way of absorbed materials of films solar cell manufacture [2, 3]. Thin films semiconducting chalcogenides have appeared as one of the most fast increasing attention of investigators in the last couple of decades especially ternary compounds because their applications in many fields of technology and science like light emitting diodes, solar cells, non-linear optical devices, electronic, sensors, optical and superconductor devices which has attracted researchers to study preparation and physical properties of these compounds [4]. Simple ternary compound CuZnS (CZS) films have a direct wide-band gap (1.6 near 2.7) eV via variable Cu to Zn percentage, high absorption coefficient, bright p type inorganics material through carrier concentration (10^{21} cm^{-3}), good efficiency, stability, cheap, and abundant [2,3]. As well as, it is a mixed structure of two metal chalcogenide CuS then ZnS film, samples by a highest %Cu can been used such absorbers layer on optoelectronic and photovoltaics apply. Whereas samples thru lower %Cu can used by way of windows buffer layers solar cell [1, 5]. Recently, copper sulfide CuS receive substantial consideration, by reason of many technology application on many fields such as solar cells, such discerning radiations filter for architecturally window then photos thermally alteration for solar energy [6-8]. The structure besides optically revisions displayed hexagonal crystal structure plus a direct band gap of 2.36eV - 2.2 eV. ZnS was significant semiconductor material thru energy gap 3.65 eV, where larger values for llII–VI compounds semiconductor, n type besides can been utilized in fabricated optoelectronic procedures, for example blue light-emitting diodes, [4, 5]. There are diverse deposition techniques used to prepared CuZnS such as chemical bath deposition (CBD)[4,9],pulsed laser deposition [10] electrochemical deposition [11], spray pyrolysis,[3,12,13] photochemical deposition,[14,15] co-

* Corresponding author: boshra.k.h@ihcoedu.uobaghdad.edu.iq
https://doi.org/10.15251/CL.2024.215.385

precipitation,[16] hydrothermal process,[17] sol gel technique,[18] and successive ionic layer absorption technique (SILAR)[5,19].

This work focuses on deposition Nano crystalline films of a ternary material Copper Zinc Sulfide ($Cu_{0.5}Zn_{0.5}S$) by vacuum evaporation method. The annealing temperatures (423,523, and 623) K effect on the structures , morphologically and optically property of these films has be description utilize XRD, SEM, AFM, and optical measurement for photovoltaic application.

2. Experimental

In this work, Ternary Copper Zinc Sulfide (CZS) alloy was prepared using the Copper Cu, Zinc Zn and Sulfide S elements with high purity (99.99%) in (0.5:0.5:1) ratio, then mix these three elements in tube of quartz under pressure of ($3*10^{-4}$ mbar), then put them in electrics oven (1320 K) aimed at six hour was higher than the melting temperature of CuS & ZnS and left to cool gradually.

The $Cu_{0.5}Zn_{0.5}S$ thin films are prepare from alloy via thermal evaporation utilized (E 306) at glasses substrate with R.T and 450±20 nm thicknesses and annealed at (423,523, and 623) K intended for 1 hour to studied the morphological, structurally, then optically property of CZS thin films. X-ray diffraction XRD technique has been used to characterized the structural of films prepared using CuKα radiation with (λ = 1.5418 Å), 20 mA current and 40Kv voltage by record 2Θ from 20° to 80 °. Bragg's law were utilize for calculated the inter planar spacing (d) of miller index (hkl) [20].

$$2d\sin\theta=n\lambda \quad (1)$$

The crystalline size (C.S) of CZS films was estimated by using Scherer's Formula [21, 22]:

$$C.S=\frac{0.94\lambda}{\beta COS\theta} \quad (2)$$

where λ: indicates the XRD wave length, β: indicates the FWHM of the peaks, and θ: indicates Bragg's angle.

The dislocations density (δ) were calculate thru used Williamson besides Smallman's equations [23]:

$$\delta = \frac{1}{(C.S)2} \quad (3)$$

While Micro strain (Ɛ) could be deliberate from equivalence [24]:

$$Ɛ=\frac{B\cos\theta}{4} \quad (4)$$

AFM were used to characterize the morphology of the films surface. Optical properties of CZS films prepare has been investigation by recorded the transmission and absorption spectrums on variety (300-1100) nm. Tauc's equation is utilize for determine the optical energy gap: [25, 26]

$$(\alpha h\nu)=D\,(h\nu - E_g) \quad (5)$$

where D: is constant, hν: the incident photon energy, n: is a number which depending on the transition type and α: the absorption coefficient which calculated from equation: [27, 28]

$$\alpha=\frac{2.303A}{t} \quad (6)$$

where A: is absorbance, t: film thickens.

The refractive index (n) values was estimated by using formula: [29]

$$n = \{[4R / (R-1)]-K^2\}^{1/2} - [(R+1) / (R-1)] \quad (7)$$

where (K) is the extinction coefficient which calculated by using equation: [30]

$$K=\frac{\alpha\lambda}{4\pi} \quad (8)$$

The reflectance (R) is calculated by: [30]

$$R = 1-T-A \quad (9)$$

Real part ε_r and imaginary part ε_i of dielectric constant could been calculated via relation below: [31, 32]

$$\varepsilon_r = n^2-K^2 \quad (10)$$

$$\varepsilon_i = 2nK \quad (11)$$

3. Results and discussions

3.1. X-ray diffraction analyses

Figure 1, demonstrations XRD analysis of $Cu_{0.5}Zn_{0.5}S$ thin films deposited with a thickness (450nm) at R.T and after annealing at (423,523,623) K for one hour. This figure indicates that wholly films prepared previously then later annealed have a polycrystalline structure with low crystallinity, hexagonal structure with mixed phase of CuS and ZnS. The XRD patterns obtained from this figures are cooperation with standards XRD references pattern of ZnS (JCPDS: 65-0309) and CuS (JCPDS: 06-0464) because there are no standard XRD reference patterns for ternary CZS compound. XRD patterns (Fig.1) show that CuS performance such a prominent phased with strongest sharp peaks corresponding to CuS standard are appeared in all films at diffraction angle 2θ (29.98°,29.89°,29.60° and 29.75°) before and after annealing respectively refer to (102) plane.

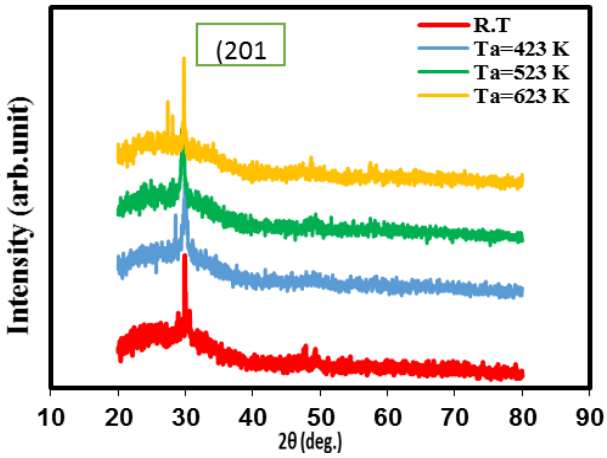

Fig. 1. XRD of $Cu_{0.5}Zn_{0.5}S$ thin films at R.T and different annealing temperatures.

Also can notice that no distinguishing peaks of Cu, Zn, or S elements are observed. Secondary peak were seemed in the XRD patterns mentions for ZnS and CuS phase, the results are in good contract with standard values (JCPDS) card file data and the peak positions change marginally after annealing. In addition, the peaks intensities increase after annealed besides crystallites size developed largest. That indicates the crystal film has been enhanced due to reduced defects and orderliness system [22]. These remarks are good agreed with ref [1,5].

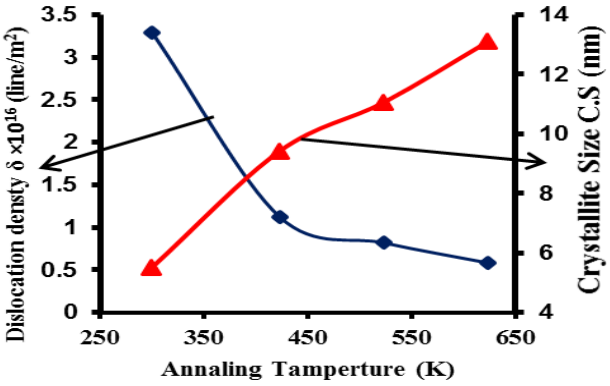

Fig. 2. (C.S) and (δ) versus annealing temperatures for CZS thin films before and after annealing.

The crystallites size(C.S), dislocations density (δ) ,and Micro strain (Ɛ) are listed in Table (1) where it shows increase crystallite size value while decrease the values of both dislocation density and micro strain with increasing annealing temperatures due to decreasing in films defects and improved crystal structure of these films. Also notice from this table and figure(2)that the $Cu_{0.5}Zn_{0.5}S$ films annealed at 623 K have high crystallite size with lower dislocations density and Micro strain for extra sample due to reductions at FWHM of main peaks where lastly lead to intensification on crystallites size of the films [33]. As well as observed that the variation in dislocation density and micro strain is inversely related to the crystallite size, this result agrees with [3].

Table 2. Structures parameter for $Cu_{0.5}Zn_{0.5}S$.

Sample	**2θ (Deg.)**	**FWHM(Deg.)**	**d_{hkl} (exp) A°**	**C.S (nm)**	**δ× 10^{16} (lines/m^2)**	Ɛ×10^{-3}
R.T	29.9833	1.56	2.97783	5.509	3.294	6.571
Ta= 423 K	29.8985	0.91	2.98608	9.422	1.1216	3.834
Ta= 523 K	29.6054	0.7767	3.01498	11.055	0.818	3.274
Ta= 623 K	29.7556	0.656	3.0010	13.093	0.583	2.764

3.2. (AFM) measurement

Surface morphology of $Cu_{0.5}Zn_{0.5}S$ thin films per thick (450nm) on R.T in addition after annealing at (423,523,623) K were examined by AFM analysis. Figure (2) shows Granularity Cumulation Distribution and 3D images of these films. From this figure we can notice that all films prepared have uniform distribution with Nano grain size packed together without any pinholes or cracks. AFM results such as roughness, root mean square and average grain size (G.S)

are shown in Table (2). These results showed clearly that average grain size various from (52.37) nm to (89.25) nm as well as all parameters are Increase after annealing and the sample annealing at 623 K have high values. This behavior is due to improvement film structure, increase atoms mobility which causes the accumulation of particles and rise film surface roughness which can play good role for thin films performance for photovoltaic cell. These observations are good agreed with XRD results and ref [2, 34].

Table 2. Surfaces roughness, Root mean square and grain size of $Cu_{0.5}Zn_{0.5}S$ at R.T and (423, 523,623) K.

Sample	Roughness (nm)	r.m.s (nm)	Grain Size (nm)
R.T	0.939	1.22	52.37
Ta= 423 K	1.54	1.93	67.17
Ta= 523 K	1.81	2.37	76.96
Ta= 623 K	4.83	6.04	89.25

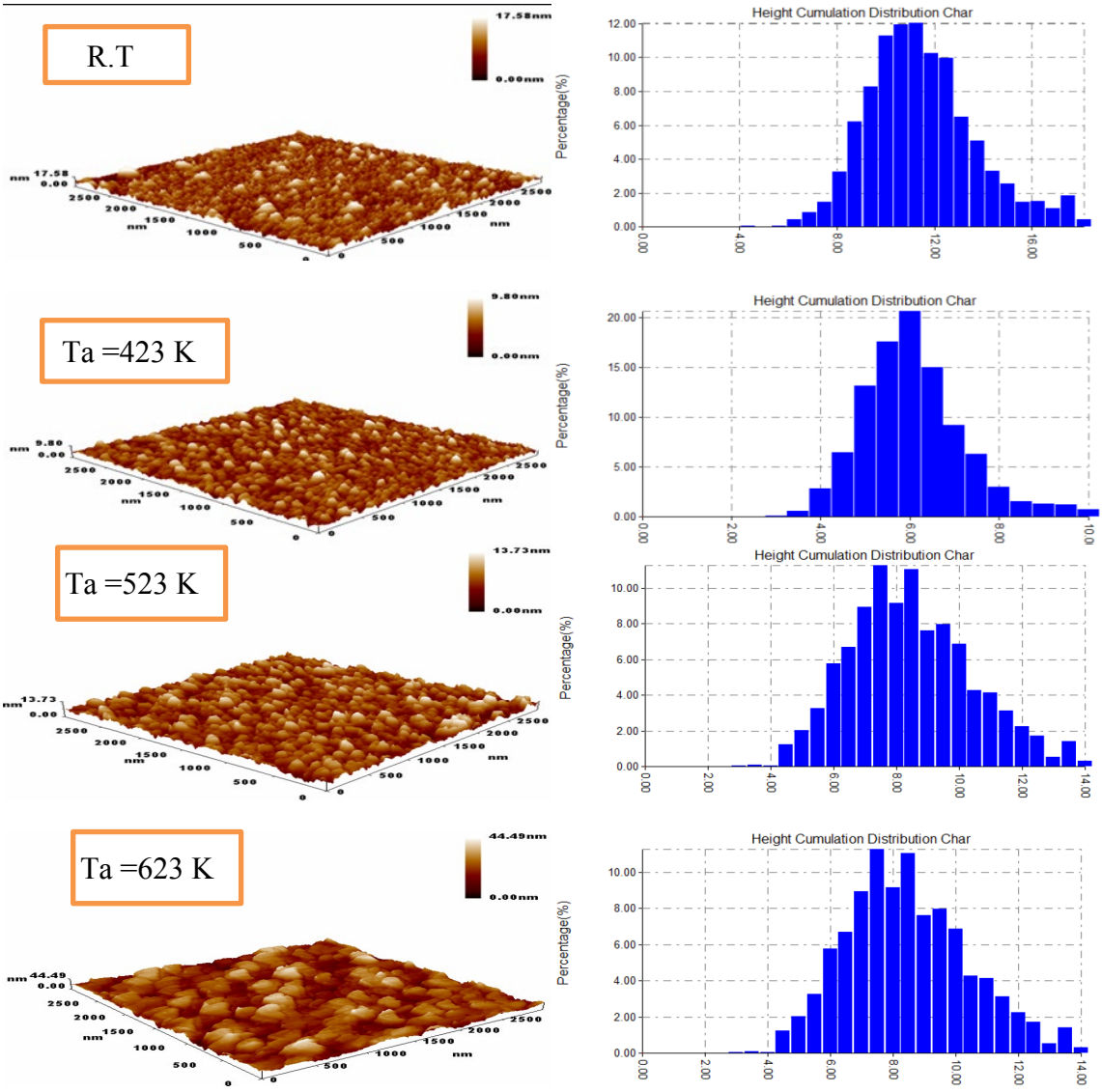

Fig. 3. AFM images of $Cu_{0.5}Zn_{0.5}S$ thin films at R.T and different annealing temperatures.

3.3. Optical measurement

The optical absorbance spectra in the wavelength range (400–1000) nm of $Cu_{0.5}Zn_{0.5}S$ thin films at R.T and after annealing at (423,523,623) K for 1 hour are displayed in Figure (4). This figure show the increase in absorbance values after annealing while decrease with increasing wave length for all films, which means decreased the transmittance values after annealing. The improvement in absorbance after annealing can been attributed towards growths the crystals size due to reduction in optical scattering which related to AFM and XRD data with the intention of understudied the association amid structure, surfaces morphology besides optical absorbance , this means the photons absorption thru free carriers donated to diminution in optical transmitted [28,34]. It can be seen from this figure the high absorbance value after annealing at 623K are proximate 90% which make $Cu_{0.5}Zn_{0.5}S$ films a favorite material for photovoltaic applications. This behavior is comparable with the study [1, 5].

The films had highest absorption coefficient ($\alpha > 10^4$ cm^{-1}) which calculated from equation (6), this means the allowed direct transition possible occur, as well as increase absorption coefficients values after annealing as shown in Figure (5) for the same reasons we mention before . Figure (6) demonstration relative $(\alpha h\upsilon)^2$ verses $h\upsilon$ for $Cu_{0.5}Zn_{0.5}S$ thin films which used to calculate the energy gap according to Tauc's equation. The results display that a reduction in the optical energy gap values from 2.4 eV to 1.9 eV shifted to lower photon energy (extended wavelength NIR area) after annealing. This behavior can be credited to the fact that the variation in grain boundaries and crystallite size when annealed could cause the variation in the optical band gap. The energy gap values for these films are good contract with [1,2,3,5], as well as would be well matched for solar cell application.

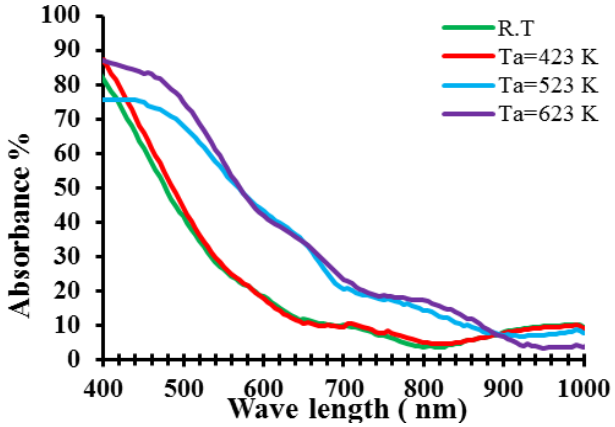

Fig. 4. Absorbance of CZS thin films versus energy wave length before and after annealing.

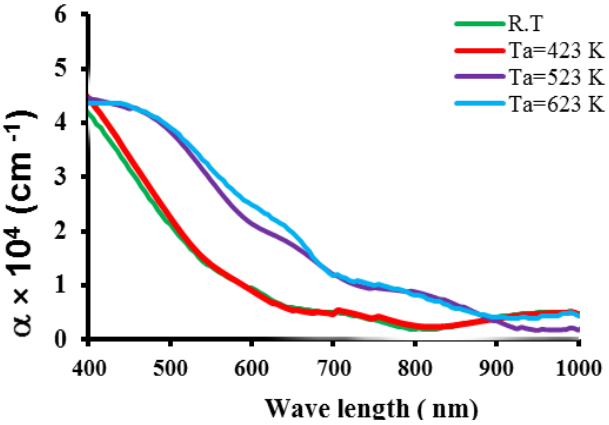

Fig. 5. Absorption coefficients versus photon for CZS thin films before and after annealing.

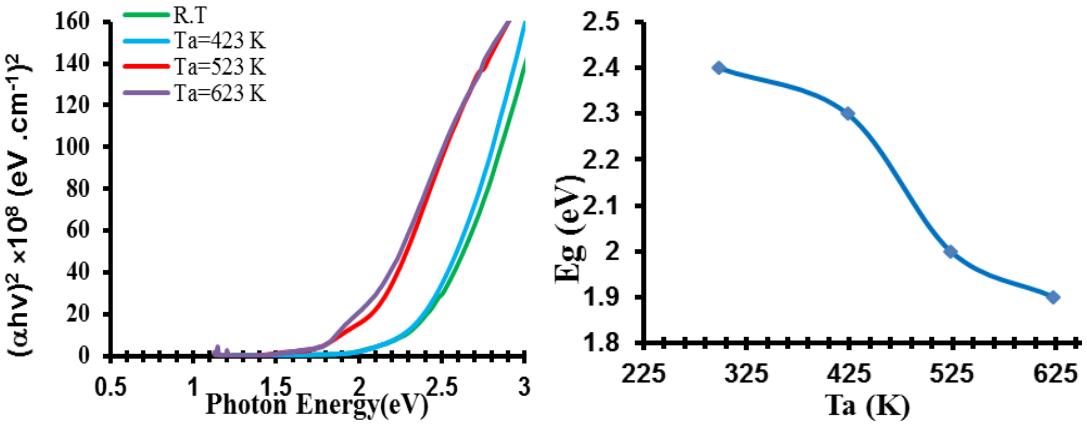

Fig. 6. Variation $(\alpha hv)^2$ with photon energy and optical energy gap for $Cu_{0.5}Zn_{0.5}S$ thin films before and after annealing.

Equation (7) was used to compute the refractive index. The variation of n for $Cu_{0.5}Zn_{0.5}S$ thin films at R.T and after annealing at (423,523,623) K is illustrated in figure (7). This figure display that, the refractive index values decrease after annealing due to changes in the structural features of films, matching with reflectance value, as well as all samples have a peak shift to lower wave length.

The extinction coefficient (k) values variation with wave length as a function of annealing temperatures for CZS films as seen in figure (8). These values increase after annealing takings similar behavior of the absorption coefficient because it mainly depends on the absorption coefficient values.

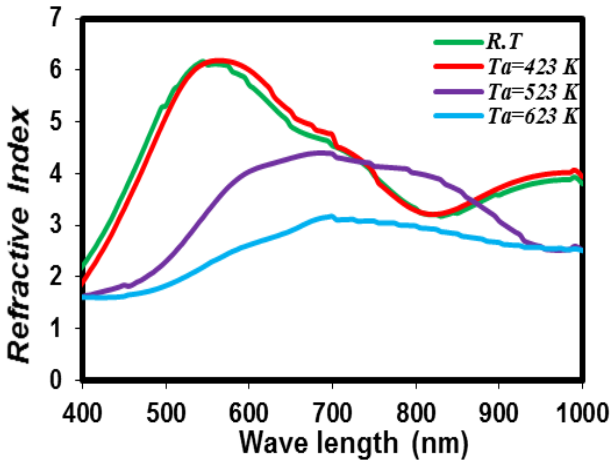

Fig. 7. Refractive index versus wave length for CZS thin films before and after annealing.

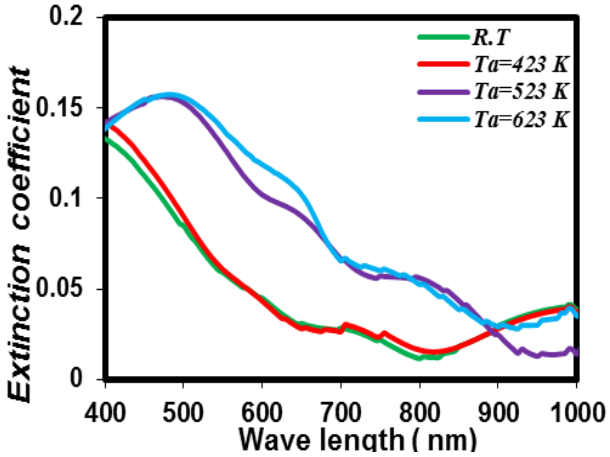

Fig 8. Extinction coefficient versus wave length for CZS thin films before and after annealing.

The complex dielectric constant which describe the fundamental electron excitation spectrum of the film by means of the frequency, explain by real (εr) and imaginary εi parts of dielectric constant. The real (εr) part take the same behavior of refractive index (n), while the imaginary εi part behavior is similar to extinction coefficient (k) because it mainly depends on n and k values respectively.

Figure (9) show the loss tangent which is calculated from the relation [23]:

$$\tan\delta = \varepsilon i / \varepsilon r \qquad (12)$$

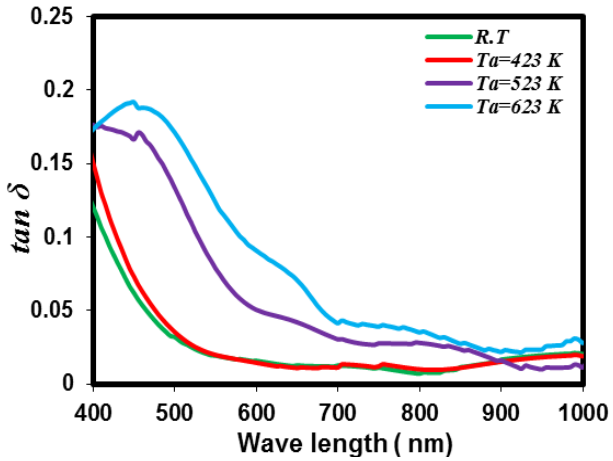

Fig. 9. Variation loss tangent with wave length for $Cu_{0.5}Zn_{0.5}S$ thin films before and after annealing.

It is clear from this figure that loss factor (tanδ) which represents the characteristic dissipation of electromagnetic energy in the material into heat, varies with wavelength from (0.01) to (0.14) depends on grain size ,structural defects , and lattice strain in the films. In this present study the optical constants before and after annealing at different temperature show in Table (3).

Table 3. The optical constants for $Cu_{0.5}Zn_{0.5}S$ at R.T and (423, 523,623) K.

Sample	Eg^{opt} (eV)	Optical parameter at λ = 550 nm				
		α x 10^4 cm^{-1}	n	K	ε_1	ε_2
R.T	**2.4**	**1.350**	**6. 18**	**0.059**	**37.309**	**0.722**
Ta= 423 K	**2.3**	**1.387**	**6.15**	**0.061**	**37.916**	**0.748**
Ta= 523 K	**2**	**2.934**	**3.26**	**0.128**	**10.672**	**0.84**
Ta= 623 K	**1.9**	**3.155**	**2.24**	**0.138**	**5.016**	**0.62**

4. Conclusion

Nano crystalline $Cu_{0.5}Zn_{0.5}S$ thin films were grown on a glass substrate with 450 nm thickness using thermal evaporation method before and after annealing at (423,523,623) K for one hour. The influence of annealing at different temperatures on structural, surface morphology and optical properties of CZS thin films were investigated. The XRD study confirms the fact that $Cu_{0.5}Zn_{0.5}S$ thin films are polycrystalline hexagonal in nature and formation mixed phase of CuS and ZnS with preferential orientation in (102) plane. The annealing temperatures played an essential role in the crystallite size which increased from 5.509 to 13.093 nm. AFM results displayed uniformly distributed and grain size increased after annealing. Optical measurement results demonstrate the high values of absorption coefficient and a direct optical energy gap reduced from 2.4 eV to 1.9 eV after annealing , indicating enhance films properties for use in photovoltaic application.

References

[1] A.H.M. Abd El-Gawad, A.A.I. Khalil, A.-S. Gadallah, Optik 223,(2020); https://doi.org/10.1016/j.ijleo.2020.165561

[2] Edwin Jose, M.C. Santhosh Kumar, Journal of Alloys and Compounds 712, 649-656, (2017); https://doi.org/10.1016/j.jallcom.2017.04.097

[3] Aabel P, Santhosh Kumar M C , Int J Energy Res. 2020;1-11.

[4] Nanasaheb P. Huse, Rohit M. Patil, Ramphal Sharma, ES Mater. Manuf., (2023), 20, 839

[5] M. AliYildirim, Aytunc- Ates, AykutAstam, Physica E 41, 1365-1372, (2009); https://doi.org/10.1016/j.physe.2009.04.014

[6] P. K. Nair, M. S. Nair, Semiconductor Science and Technology, 1992, 7, 239-244; https://doi.org/10.1088/0268-1242/7/2/011

[7] M. Ali Yıldırım, Optics Communications, 2012, 285, 1215-1220; https://doi.org/10.1016/j.optcom.2011.10.062

[8] K. Yang, M. Ichimura, Japanese Journal of Applied Physics, 2011, 50, 040202; https://doi.org/10.1143/JJAP.50.040202

[9] G. M. M. Gubari, S. M. Ibrahim Mohammed, N. P. Huse, A. S. Dive, R. Sharma, Journal of Electronic Materials, 2018, 47, 6128-6135; https://doi.org/10.1007/s11664-018-6491-3

[10] A. M. Diamond, L. Corbellini, K. R. Balasubramaniam, S. Chen, S. Wang, T. S. Matthews, L.-W. Wang, R. Ramesh, J. W. Ager, Physica Status Solidi (A), 2012, 209, 2101-2107; https://doi.org/10.1002/pssa.201228181

[11] K. Yang, Y. Nakashima, M. Ichimura, Journal of the Electrochemical Society, 2012, 159, H250-H254; https://doi.org/10.1149/2.042203jes

[12] M. Adelifard, H. Eshghi, M. M. Bagheri Mohagheghi, Optics Communications, 2012, 285, 4400-4404; https://doi.org/10.1016/j.optcom.2012.06.030
[13] M. S. Sreejith, D. R. Deepu, C. S. Kartha, K. Rajeevkumar, K. P. Vijayakumar, Applied Physics Letters, 2014, 105, 202107; https://doi.org/10.1063/1.4902224
[14] D. Man, Y. Kai, M. Ichimura, Semiconductor Science and Technology, 2012, 27, 125007; https://doi.org/10.1088/0268-1242/27/12/125007
[15] M. Ichimura, Y. Maeda, Solid-State Electronics, 2015, 107, 8-10; https://doi.org/10.1016/j.sse.2015.02.016
[16] V. Laxminarasimha Rao, T. Shekharam, T. Mohan Kumar, M. Nagabhushanam, Materials Chemistry and Physics, 2015, 159, 83-92; https://doi.org/10.1016/j.matchemphys.2015.03.055
[17] X.-H. Guan, P. Qu, X. Guan, G.-S. Wang, RSC Advances, 2014, 4, 15579-15585; https://doi.org/10.1039/C4RA00659C
[18] W.-S. Ni, Y.-J. Lin, Applied Physics A, 2015, 119, 1127-1132; https://doi.org/10.1007/s00339-015-9079-2.
[19] M, A. Yildirim, Physica E: Low-Dimensional Systems and Nanostructures, 2009, 41, 1365-1372; https://doi.org/10.1016/j.physe.2009.04.014
[20] Abbas Haider H. AL-Obeidi, Bushra K. H. Al-Maiyaly, AIP Conference Proceedings 2475, 090026 (2023); https://doi.org/10.1063/5.0123128
[21] Duaa Muneer Sadiq, Bushra K. H. Al-Maiyaly, Ibn Al-Haitham J. for Pure & Appl. Sci., 36 (2), 113-123 (2023); https://doi.org/10.30526/36.2.2930
[22] A. A. Hamid, Bushra K. H. Al-Maiyaly, Chalcogenide Letters 19, (9), p. 579 - 590,(2022); https://doi.org/10.15251/CL.2022.199.579
[23] Ghuzlan Sarhan Ahmed, Bushra K. H. Al-Maiyaly, AIP Conference Proceedings 2123, 020074 (2019); https://doi.org/10.1063/1.5117001
[24] R. H. Athab and B. H. Hussein, Digest Journal of Nanomaterials and Biostructures, 17, 4, 1173-1180, (2022); https://doi.org/10.15251/DJNB.2022.174.1173
[25] Bushra H. Hussein, Hanan K. Hassun, Neuro Quantology 18(5), 77 (2020).
[26] B. K. H. AL-Maiyal, B. H. Hussein, H. K. Hassun, Journal of Ovonic Research, 16 (5), 267-271 (2020); https://doi.org/10.15251/JOR.2020.165.267
[27] Bushra K. Hassoon Al-Maiyaly, Ibn Al-Haitham J. for Pure & Appl. Sci., 29 (3), 14-25 (2016).
[28] Sa. M. Ali, H. K. Hassun, A. A. Salih, R. H. Athabb, B. K. H. Al-Maiyaly, B. H. Hussein, Chalcogenide Letters, 19 (10), 663-671, (2022); https://doi.org/10.15251/CL.2022.1910.663
[29] B. K. H. AL-Maiyal, Ibn Al-Haitham J. for Pure & Appl. Sci 26(1) (2013).
[30] B. K. H. AL-Maiyal, Ibn Al-Haitham J. for Pure & Appl. Sci, 28 (3) (2015).
[31] S.Sze and K.Ng., Physics of Semiconductor Devices, 3rd edition, John Wiley and Sons, 2007; https://doi.org/10.1002/0470068329
[32] Hassun, H.K., Al-Maiyaly, B.K.H., Hussein, B.H., Moussa, Y.K.H. Journal of Ovonic Research, 19(6), 719–726 (2023); https://doi.org/10.15251/JOR.2023.196.719
[33] H. I. Mohammed, I. H. Khdayer, I. S. Naji, Chalcogenide Letters, 17 (3) 107-115 (2020); https://doi.org/10.15251/CL.2020.173.107
[34] G. H. C. Radloff, F. M. Naba, D. B. Ocran-Sarsah, M. E. Bennett, K. M. Sterzinger, A. T. Armstrong, O. Layne, M. B. Dawadi, Digest Journal of Nanomaterials and Biostructures 17 (2) 457 - 472 (2022).